

Measurement of the  $\tau^0$  lifetime

The SELEX Collaboration

M. Iori<sup>r</sup>, A. S. Ayan<sup>p</sup>, U. Akgun<sup>p</sup>, G. Alkhozov<sup>k</sup>,  
 J. Amaro-Reyes<sup>m</sup>, A. G. Antochouk<sup>k;1</sup>, M. Y. Balatz<sup>h;1</sup>,  
 A. Blanco-Covarrubias<sup>m</sup>, N. F. Bondar<sup>k</sup>, P. S. Cooper<sup>e</sup>,  
 L. J. Dauwe<sup>q</sup>, G. V. Davidenko<sup>h</sup>, U. Dersch<sup>i;2</sup>,  
 A. G. Dolgolenko<sup>h</sup>, G. B. Dzyubenko<sup>h</sup>, R. Edelstein<sup>c</sup>,  
 L. Emmediato<sup>s</sup>, A. M. F. Endler<sup>d</sup>, J. Engelfried<sup>m;3</sup>, I. Eschrich<sup>i;3</sup>,  
 C. O. Escobar<sup>s;4</sup>, A. V. Evdokimov<sup>h</sup>, I. S. Filimonov<sup>j;1</sup>,  
 F. G. Garcia<sup>s;e</sup>, M. Gaspero<sup>r</sup>, I. Giller<sup>`</sup>, V. L. Golovtsov<sup>k</sup>,  
 P. Gouon<sup>s</sup>, E. Gumez<sup>b</sup>, H. E. Kangling<sup>g</sup>, S. Y. Jun<sup>c</sup>,  
 M. Kaya<sup>p;5</sup>, J. Kimer<sup>e</sup>, V. T. Kim<sup>k</sup>, L. M. Kochenda<sup>k</sup>,  
 I. Konorov<sup>i;6</sup>, A. P. Kozhevnikov<sup>f</sup>, A. G. Krivshich<sup>k</sup>,  
 H. Kuger<sup>i;7</sup>, M. A. Kubantsev<sup>h</sup>, V. P. Kubarovsky<sup>f</sup>,  
 A. I. Kulyavtsev<sup>c;e</sup>, N. P. Kuropatkin<sup>k;e</sup>, V. F. Kurshetsov<sup>f</sup>,  
 A. Kushnirenko<sup>c;f</sup>, S. Kwan<sup>e</sup>, J. Lach<sup>e</sup>, A. Lambert<sup>t</sup>,  
 L. G. Landsberg<sup>f;1</sup>, I. Larin<sup>h</sup>, E. M. Leikin<sup>j</sup>, Li Yunshan<sup>g</sup>,  
 M. Luksys<sup>n</sup>, T. Lungov<sup>s</sup>, V. P. Malcev<sup>k</sup>, D. Mao<sup>c;8</sup>,  
 Mao Chensheng<sup>g</sup>, Mao Zhenlin<sup>g</sup>, P. M. Athew<sup>c;9</sup>, M. Mattson<sup>c</sup>,  
 V. M. Atveev<sup>h</sup>, E. M. Clement<sup>p</sup>, M. A. Moinester<sup>`</sup>,  
 V. V. Molchanov<sup>f</sup>, A. Morelos<sup>m</sup>, K. D. Nelson<sup>p;10</sup>,  
 A. V. Nemitskin<sup>j</sup>, P. V. Neoustroev<sup>k</sup>, C. Newson<sup>p</sup>, A. P. Nilov<sup>h;1</sup>,  
 S. B. Nunushev<sup>f</sup>, A. Ocherashvili<sup>`;11</sup>, Y. Onel<sup>p</sup>, E. Ozel<sup>p</sup>,  
 S. Ozkonuklu<sup>p;12</sup>, A. Penzo<sup>t</sup>, S. V. Petrenko<sup>f</sup>, P. Pogodin<sup>p;13</sup>,  
 M. Procaro<sup>c;14</sup>, V. A. Putskoi<sup>h</sup>, E. Ramberg<sup>e</sup>,  
 G. F. Rappazzo<sup>t</sup>, B. V. Razmyslovich<sup>k;15</sup>, V. I. Rud<sup>j</sup>, J. Russ<sup>c</sup>,  
 P. Schiavon<sup>t</sup>, J. Simon<sup>i;16</sup>, A. I. Sitnikov<sup>h</sup>, D. Skow<sup>e</sup>,  
 V. J. Smith<sup>o</sup>, M. Srivastava<sup>s</sup>, V. Steiner<sup>`</sup>, V. Stepanov<sup>k;15</sup>,  
 L. Stutte<sup>e</sup>, M. Svoiski<sup>k;15</sup>, N. K. Terentyev<sup>k;c</sup>, G. P. Thomas<sup>a</sup>,  
 I. Torres<sup>m</sup>, L. N. Uvarov<sup>k</sup>, A. N. Vasiliev<sup>f</sup>, D. V. Vavilov<sup>f</sup>,  
 E. Vazquez-Jauregui<sup>m</sup>, V. S. Verébryusov<sup>h</sup>, V. A. Victorov<sup>f</sup>,

V. E. Vishnyakov<sup>h</sup>, A. A. Vorobyov<sup>k</sup>, K. Vorwalter<sup>i,l,7</sup>, J. You<sup>c,e</sup>,  
Zhao Wenheng<sup>g</sup>, Zheng Shuchen<sup>g</sup>, R. Zukanovich-Funchal<sup>s</sup>

<sup>a</sup>Ball State University, Muncie, IN 47306, U.S.A.

<sup>b</sup>Bogazici University, Bebek 80815 Istanbul, Turkey

<sup>c</sup>Carnegie-Mellon University, Pittsburgh, PA 15213, U.S.A.

<sup>d</sup>Centro Brasileiro de Pesquisas Físicas, Rio de Janeiro, Brazil

<sup>e</sup>Fermi National Accelerator Laboratory, Batavia, IL 60510, U.S.A.

<sup>f</sup>Institute for High Energy Physics, Protvino, Russia

<sup>g</sup>Institute of High Energy Physics, Beijing, P.R. China

<sup>h</sup>Institute of Theoretical and Experimental Physics, Moscow, Russia

<sup>i</sup>Max-Planck-Institut für Kernphysik, 69117 Heidelberg, Germany

<sup>j</sup>Moscow State University, Moscow, Russia

<sup>k</sup>Petersburg Nuclear Physics Institute, St. Petersburg, Russia

<sup>l</sup>Tel Aviv University, 69978 Ramat Aviv, Israel

<sup>m</sup>Universidad Autónoma de San Luis Potosí, San Luis Potosí, Mexico

<sup>n</sup>Universidade Federal da Paraíba, Paraíba, Brazil

<sup>o</sup>University of Bristol, Bristol BS8 1TL, United Kingdom

<sup>p</sup>University of Iowa, Iowa City, IA 52242, U.S.A.

<sup>q</sup>University of Michigan-Flint, Flint, MI 48502, U.S.A.

<sup>r</sup>University of Rome "La Sapienza" and INFN, Rome, Italy

<sup>s</sup>University of São Paulo, São Paulo, Brazil

<sup>t</sup>University of Trieste and INFN, Trieste, Italy

---

Abstract

We report a precise measurement of the  $\Lambda_c^0$  lifetime. The data were taken by the SELEX (E781) experiment using 600 GeV  $e^+e^-$  and p beam s. The measurement has been made using 83  $\Lambda_c^0$  reconstructed in the  $\Lambda_c^0 \rightarrow \Lambda^0 \pi^+$  and  $\Lambda_c^0 \rightarrow \Sigma^0 \pi^+$  decay modes. The lifetime of the  $\Lambda_c^0$  is measured to be  $65 \pm 13$  (stat)  $\pm 9$  (sys) fs.

Key words: Charm baryon lifetime

PACS: 14.20.Lq, 13.30.-a

---

## 1 Introduction

Several experiments [1,2,3,4,5,6] in the last years have detected the  $\chi_c^0$  ground state as well as an excited state. Recently at Fermilab the photoproduction experiment, FOCUS, reported an observation of a sample of 64  $\chi_c^0$  events and they measured its lifetime as  $72 \pm 13 \pm 11$  fs [7]. The experiment WA89 published an  $\chi_c^0$  lifetime measurement of  $55^{+13}_{-11} +^{18}_{-23}$  fs from a sample of 86 events [8]. The present world average is  $69 \pm 12$  fs as reported in Ref. [9]. Clearly additional measurements of lifetime as well as the branching ratios with more statistical accuracy are needed to test theoretical models [10,11].

In this letter we report the results of a new measurement of the lifetime based on data from the hadroproduction experiment SELEX (E781) at Fermilab. The measurement is based on a sample of  $83 \pm 19$  fully reconstructed  $\chi_c^0$  from  $15.3 \pm 10^9$  hadronic interactions.

The SELEX detector at Fermilab is a 3-stage magnetic spectrometer. The negatively charged 600 GeV/c beam contains nearly equal fractions of  $\pi^-$  and  $K^-$ . The positive beam contains 92% protons. Beam particles are identified as a baryon or a pion by a transition radiation detector. The spectrometer was designed to study charm production in the forward hemisphere with good mass and decay vertex resolution for charm momenta in the range 100–500 GeV/c. Five interaction targets (2 Cu and 3 C) have a total target

---

Corresponding author.

Email address: jurgen@ifisica.uaslp.mx (J.Engelfried).

<sup>1</sup> deceased

<sup>2</sup> Present address: Advanced Mask Technology Center, Dresden, Germany

<sup>3</sup> Present address: University of California at Irvine, Irvine, CA 92697, USA

<sup>4</sup> Present address: Instituto de Física da Universidade Estadual de Campinas, UNICAMP, SP, Brazil

<sup>5</sup> Present address: Kafkas University, Kars, Turkey

<sup>6</sup> Present address: Physik-Department, Technische Universität München, 85748 Garching, Germany

<sup>7</sup> Present address: The Boston Consulting Group, München, Germany

<sup>8</sup> Present address: Lucent Technologies, Naperville, IL

<sup>9</sup> Present address: Baxter Healthcare, Round Lake IL

<sup>10</sup> Present address: University of Alabama at Birmingham, Birmingham, AL 35294

<sup>11</sup> Present address: NRCN, 84190 Beer-Sheva, Israel

<sup>12</sup> Present address: Süleyman Demirel Üniversitesi, Isparta, Turkey

<sup>13</sup> Present address: Legal Department, Oracle Corporation, Redwood Shores, California

<sup>14</sup> Present address: DOE, Germantown, MD

<sup>15</sup> Present address: Solidum, Ottawa, Ontario, Canada

<sup>16</sup> Present address: Siemens Medizintechnik, Erlangen, Germany

<sup>17</sup> Present address: Allianz Insurance Group IT, München, Germany

thickness of  $4.2\% \lambda_{\text{int}}$  for protons. The targets are spaced by  $1.5\text{ cm}$ . Downstream of the targets there are 20 Silicon Strip Detectors (SSD) with a strip pitch of  $20\text{--}25\text{ }\mu\text{m}$  oriented in X, Y, U and V views. The first spectrometer level has three Multi-Wire Proportional Chambers (MWPC) with  $3\text{ mm}$  wire spacing and  $2\text{--}2\text{ m}^2$  area downstream of bending magnet M1. The second spectrometer level has 7 MWPCs with  $2\text{ mm}$  wire spacing downstream of the second bending magnet M2. Each chamber has two sensitive planes in two orthogonal projections. The scattered-particle spectrometers have momentum cutoffs of  $2.5\text{ GeV}/c$  and  $15\text{ GeV}/c$  respectively. Typical momentum resolution for a  $100\text{ GeV}/c$  track is  $0.5\%$ . A Ring-Imaging Cherenkov detector (RICH) [12], filled with Neon at room temperature and pressure, provides single track ring radius resolution of  $1.4\%$  and  $2\text{--}K =$  separation up to about  $165\text{ GeV}/c$ . A layout of the spectrometer can be found elsewhere [13].

## 2 Reconstruction of hyperons $\Lambda$ , $\Sigma$ and $\Xi$

The  $\Lambda^0$  decays studied here have a hyperon in the final state. Hyperons that decay upstream of or within the M1 magnet are called Kink tracks. They are characterized by one charged track that decays to another charged particle and a neutral particle undetected by the spectrometer. Such Kink tracks differ from the majority of spectrometer tracks in that the vertex silicon track segment does not link to straight line tracks segments measured in the spectrometers after M1 and/or M2. The Kink reconstruction algorithm examines all unlinked Vertex SSD track segments that point to the M1 magnet aperture and tries to match each unlinked segment with an unlinked downstream track measured in the M1/M2 spectrometer, using momentum-energy conservation with the hypothesis of a specific hyperon decay. The momentum of the parent hyperon ( $\Lambda$ ,  $\Sigma$  or  $\Xi$ ) is calculated using the assumed decay hypothesis. The daughter Kink in decays must be RICH identified with the likelihood to be a Kink exceeding that of its being a  $\Lambda$ .

## 3 Data set and charm selection

The charm trigger is very loose. It requires a valid beam track, at least 4 charged secondaries in the forward  $150\text{ mrad}$  cone, and two hodoscope hits after the second bending magnet from tracks of charge opposite to that of the beam. We triggered on about  $1/3$  of all inelastic interactions. A computational filter linked MWPC tracks having momenta  $> 15\text{ GeV}/c$  to hits in the vertex silicon and made a full reconstruction of these tracks together with a beam track to form primary and secondary vertices in the event. Events consistent

with only a primary vertex are not saved. About 1/8 of all triggers are written to tape, for a final sample of about  $10^9$  events.

In the full analysis the vertex reconstruction was repeated with tracks of all momenta. The RICH detector identified charged tracks above  $25 \text{ GeV}/c$ . Results reported here come from a second pass reconstruction through the data, using a production code optimized for hyperon reconstruction.

To separate the signal from the non-charm background we require that: (i) the spatial separation  $L$  between the reconstructed production and decay vertices exceeds 6 times the combined error  $\sigma_L$ , (ii) each decay track, extrapolated to the primary vertex  $z$  position, must miss by a transverse distance  $s \geq 2.5$  times its error  $\sigma_s$ , (iii) each candidate hyperon track, extrapolated to the  $K$  vertex  $z$  position, must have a good vertex quality ( $\chi^2/\text{NDOF} < 5$ ), (iv) the secondary vertex must lie outside any target material by at least  $0.05 \text{ cm}$ , and (v) decays must occur within a fiducial region.

The total transverse momentum of pions from the  $\Lambda^0 \rightarrow p \pi^-$  decay mode must be greater than  $0.35 \text{ GeV}/c$  with respect to the  $\hat{z}_c$  direction. This cut optimizes the signal to background ratio. We require a minimum momentum of  $8 \text{ GeV}/c$  to reduce the number of fake invariant mass combinations. There are  $107 \pm 22$   $\Lambda^0$  candidates in three decay channels:  $\Lambda^0 \rightarrow p \pi^-$ ,  $\Lambda^0 \rightarrow n \pi^0$ , and  $\Lambda^0 \rightarrow K^+ \pi^-$ . Details of the  $\Lambda^0$  mass measurement will be reported elsewhere [14]. In the  $\Lambda^0 \rightarrow K^+ \pi^-$  mode the signal is small and the signal to noise ratio is poor. We've chosen not to include it in the lifetime measurement. The invariant mass distributions with tighter cuts for lifetime measurement are shown in Fig. 1 for the two decay modes used here.

#### 4 Lifetime evaluation using a maximum likelihood fit

The average combined error  $\sigma_L$  on the primary and secondary vertices and the average  $\Lambda^0$  momentum give a proper time resolution of  $16 \text{ fs}$ , about 23% of  $\tau_{\Lambda^0}$ . We used a binned maximum likelihood fitting technique with  $5 \text{ fs}$  width bins to determine the  $\Lambda^0$  lifetime. The fit was applied to a reduced proper time distribution,  $t = M(L - L_{\text{min}})/\beta c$  where  $M$  is the reconstructed charm mass,  $\beta$  the reconstructed momentum,  $L$  the measured vertex separation and  $L_{\text{min}}$  the minimum  $L$  for each event to pass all the imposed selection cuts.  $L_{\text{min}}$  is determined event-by-event, along with the acceptance, by the procedure described below. We fitted all events with  $t < 600 \text{ fs}$  in the mass range  $2.685 \text{ GeV}/c^2 < M(\Lambda^0) < 2.725 \text{ GeV}/c^2$ ,  $\pm 2.5$  from the  $\Lambda^0$  central mass value.

The probability density function is:

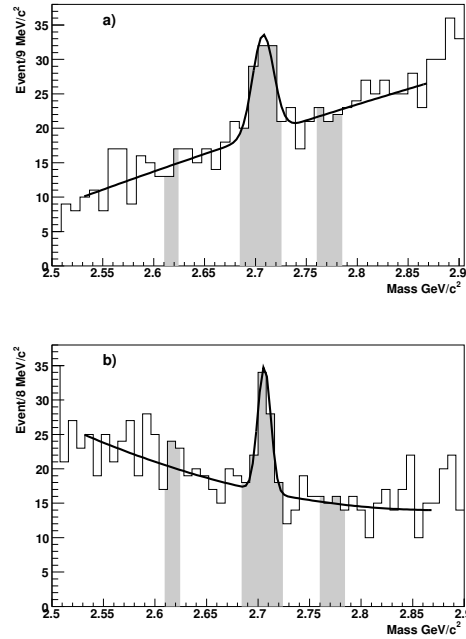


Fig.1. Invariant mass distribution for (a)  $D_c^0 \rightarrow \pi^+ K^+$ , (b)  $D_c^0 \rightarrow \pi^+ \pi^+$ . The shaded regions show the  $D_c^0$  signal and sideband regions.

$$f(M; \tau; \tau_{B1}; \tau_{B2}; f_B; f_C; t) = (1 - f_B) N_S \frac{e^{-t/\tau}}{\tau} + f_B N_S B(t) \quad (1)$$

where

$$B(t) = f_C \frac{e^{-t/\tau_{B1}}}{\tau_{B1}} + (1 - f_C) \frac{e^{-t/\tau_{B2}}}{\tau_{B2}} \quad (2)$$

The free parameters are:  $\tau$  ( $D_c^0$  lifetime),  $\tau_{B1}$ ,  $\tau_{B2}$  (background lifetimes),  $f_B$  (background fraction in the signal region) and  $f_C$  (background splitting function).  $N_S$  is the total number of events in the signal region.

The function is the sum of a term for the  $D_c^0$  exponential decay corrected by the acceptance function  $\mathcal{A}(t)$  plus a background function  $B(t)$  consisting of two exponentials to describe the strong decays and charm decays respectively. Its parameters were determined from the  $t$  distribution from the  $D_c^0$  sidebands. Together the mass widths of the sideband background windows,  $2.610 \text{ GeV} = c^2 < M(D_c^0) < 2.625 \text{ GeV} = c^2$  and  $2.760 \text{ GeV} = c^2 < M(D_c^0) < 2.785 \text{ GeV} = c^2$  was equal to the signal mass window.

The proper-time-dependent acceptance  $\mathcal{A}(t)$  is independent of spectrometer features after the first magnet, e.g., RICH efficiency and tracking efficiency. These efficiencies affect only the overall number of events detected. The proper

Table 1

Lifetime  $\tau$  results for the two  $D^0_c$  decay modes analyzed. The errors are only statistical. The signal yields from the fits to the mass plots in Fig. 2 are also shown.

Fit results	$D^0_c \rightarrow \pi^+ \pi^+$	$D^0_c \rightarrow \pi^+ \pi^0$
$\tau_c$ [fs]	62:6 22:0	65:8 16:0
$\tau_{B1}$ [fs]	15:6 6:2	10:1 3:3
$\tau_{B2}$ [fs]	388:2 27:0	281:4 22:5
Signal	34 12	23 9
background	84 13	81 6
Signal yield	47 16	36 11

time distribution of these events depends crucially on vertex reconstruction. To evaluate  $\tau(t)$  we generated  $D^0_c$  events with a  $(1 - x_F)^3$  distribution and decayed them using the QQ package [15]. We embedded these generated decays into real data events and reconstructed the embedded decays with the online package including multiple Coulomb scattering in the spectrometer and the measured detector performance. The correction function was evaluated as the fraction of the embedded events passing the selection cuts.

Figure 2 shows the overall fits to the data distributions as a function of reduced proper time for  $\pi^+ \pi^+$  and  $\pi^+ \pi^0$  decay modes. It also shows the acceptance function  $\tau(t)$ , which does not differ significantly from unity and is constant. This is due to the fact  $L_{min}$  is chosen 6 times the combined error  $\sigma_L$ . With SELEX's very high momentum and excellent resolution this cut removes only the first 1.5 lifetimes from the sample.

Table 1 summarizes the lifetime  $\tau$  results and the signal yields. We measure an average lifetime  $65 \pm 13$  fs. The uncertainties are statistical only, evaluated where  $\ln L$  increases by 0.5.

## 5 Systematic errors

The systematic uncertainties for the  $D^0_c$  lifetime analysis are listed in Table 2 and described below. Lifetime shifts due to reconstruction errors have been well studied in our  $D^0$  and  $D^0_c$  work, with an order of magnitude higher statistics [16,17]. Because of the high redundancy and good precision of the silicon vertex detector, vertex measurement effects are small at all momenta. Proper time assignment depends on correct momentum determination. The SELEX momentum error is less than 0.5% in all cases. We assign a maximum systematic error from proper time measurement of 1 fs. The acceptance

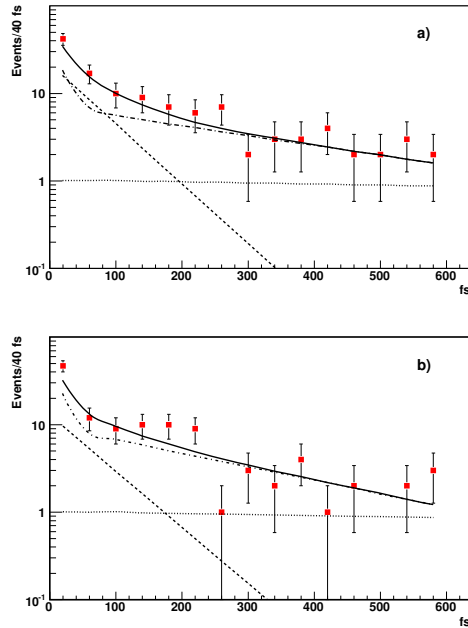


Fig. 2. Corrected reduced proper time distribution for events in the  $B_c^0$  window  $2706 < 20 \text{ M eV} = c^2$  (fullboxes) and the results from the maximum likelihood fit (solid curve) for a)  $B_c^0 \rightarrow \pi^+ \pi^-$ ; b)  $B_c^0 \rightarrow \pi^+ \pi^0$ . The dashed curve shows the  $B_c^0$  proper lifetime, the dashed-dot curve the fitted background and the dotted curve the acceptance.

Table 2

Systematic error contributions in fs for the two  $B_c^0$  decay modes analyzed.

Source of uncertainty	$B_c^0 \rightarrow \pi^+ \pi^-$ , $B_c^0 \rightarrow \pi^+ \pi^0$
Vertex reconstruction	< 1 fs
Acceptance function	1.75 fs
Fit procedure	8.5 fs
Total systematic error	8.6 fs

function used in the fit was parameterized with a 1st and 2nd order polynomial. The difference in lifetime result is 1.75 fs. No significant difference in the lifetime correction function was found when we changed the  $n$  value of the  $x_F$  distribution from 3 to 1. We varied the width of the sidebands and the bin size independently. The systematic error due to the fit procedure is 8.5 fs.

## 6 Conclusions

We have made a new measurement of the  $B_c^0$  lifetime in two independent decay channels,  $B_c^0 \rightarrow \pi^+ \pi^-$ ,  $B_c^0 \rightarrow \pi^+ \pi^0$ , using a maximum likelihood fit. SELEX

measures the  $\tau_c^0$  lifetime to be  $\tau_c^0 = 65 \pm 13$  (stat)  $\pm 9$  (sys) fs. Our result is in excellent agreement with the world average [9] and with the recent results published by the FOCUS collaboration [7].

#### Acknowledgment

The authors are indebted to the staff of Fermi National Accelerator Laboratory and for invaluable technical support from the staffs of collaborating institutions. This project was supported in part by Bundesministerium für Bildung, Wissenschaft, Forschung und Technologie, Consejo Nacional de Ciencia y Tecnología (CONACYT), Conselho Nacional de Desenvolvimento Científico e Tecnológico, Fondo de Apoyo a la Investigación (UASLP), Fundação de Amparo a Pesquisa do Estado de São Paulo (FAPESP), the Secretaría de Educación Pública (Mexico) (grant number 2003-24-001-026), the Israel Science Foundation founded by the Israel Academy of Sciences and Humanities, Istituto Nazionale di Fisica Nucleare (INFN), the International Science Foundation (ISF), the National Science Foundation (Phys # 9602178), NATO (grant CR 6.941058-1360/94), the Russian Academy of Science, the Russian Ministry of Science and Technology, the Russian Foundation for Basic Research: RFBR grant 05-02-17869, the Turkish Scientific and Technological Research Board (TUBİTAK), the U.S. Department of Energy (DOE grant DE-FG 02-91ER 40664 and DOE contract number DE-AC 02-76CH O 3000), and the U.S.-Israel Binational Science Foundation (BSF).

#### References

- [1] J. Stieve, AIP Conf. Proc. 272 (1993) 1076.
- [2] P. L. Frabetti et al. [E 687 Collaboration], Phys. Lett. B 338 (1994) 106.
- [3] P. L. Frabetti et al. [E 687 Collaboration], Phys. Lett. B 300 (1993) 190.
- [4] D. Cronin-Hennessy et al. [CLEO Collaboration], Phys. Rev. Lett. 86 (2001) 3730 [arXiv:hep-ex/0010035].
- [5] P. L. Frabetti et al. [E 687 Collaboration], Phys. Lett. B 357 (1995) 678.
- [6] B. Aubert et al. [BABAR Collaboration], Phys. Rev. Lett. 97 (2006) 232001 [arXiv:hep-ex/0608055].
- [7] J. M. Link et al. [FOCUS Collaboration], Phys. Lett. B 561 (2003) 41 [arXiv:hep-ex/0302033].
- [8] M. I. Adamovich et al. [WA89 Collaboration], Phys. Lett. B 358 (1995) 151 [arXiv:hep-ex/9507004].

- [9] W .M . Yao et al. [Particle Data Group], *J. Phys. G* 33 (2006) 1.
- [10] S. Bianco, F. L. Fabbri, D. Benson and I. Biggi, *Riv. Nuovo Cim.* 26N 7 (2003) 1 [arXiv:hep-ex/0309021].
- [11] H. Y. Cheng, *Phys. Lett. B* 289 (1992) 455.
- [12] J. Engelfried et al. [SELEX Collaboration], *Nucl. Instrum. Meth. A* 431 (1999) 53 [arXiv:hep-ex/9811001].
- [13] J.S. Russ et al. [SELEX Collaboration], in *Proceedings of the 29th International Conference on High Energy Physics, 1998*, edited by A. Astbury et al. (World Scientific, Singapore, 1998) Vol. II, p. 1259 [arXiv:hep-ex/9812031].
- [14] SELEX Collaboration, to be published.
- [15] <http://www.lns.cornell.edu/public/CLEO/soft/QQ/>
- [16] A.Y. Kushnirenko, Ph.D. Thesis, Carnegie Mellon University, 2000 (unpublished). FERMILAB-THESIS-2000-09.
- [17] A. Kushnirenko et al. [SELEX Collaboration], *Phys. Rev. Lett.* 86 (2001) 5243 [arXiv:hep-ex/0010014].